Pergamon

SCIENCE DIRECT®

Tetrahedron 59 (2003) 4011–4015

TETRAHEDRON

Aggregation properties of oligo(methacrylic acid)-shelled dendrimer and its microenvironment in aqueous solutions

Masazo Niwa,* Tetsuya Higashizaki and Nobuyuki Higashi*

Department of Molecular Science & Technology, Faculty of Engineering, Doshisha University, Kyo-tanabe, Kyoto 610-0321, Japan

Received 14 October 2002; revised 24 January 2003; accepted 4 February 2003

Abstract—A third-generation poly(amido amine) dendrimer having poly(methacrylic acid) segments on the periphery (G3-PMAA) was newly synthesized. A xanthate-modified dendrimer (G3-X) was first prepared by condensation of the terminal amino groups of the poly(amido amine) dendrimer with an activated-ester xanthate. G3-PMAA was then synthesized by polymerization of methacrylic acid initiated with G3-X. The number-average degree of polymerization of PMAA segment was estimated to be 10. The pK_a value for G3-PMAA was evaluated to be 7.3 that is somewhat higher than that (6.8) of the corresponding linear PMAA with the same segment length, indicating the interaction of PMAA segments caused by assembling them at the dendrimer surface. When the diameter of G3-PMAA in aqueous solution at various pHs was measured by a dynamic light scattering, G3-PMAA was found to self-aggregate in a pH region, where the PMAA segment took a hydrophobic, compact coil conformation. Subsequently, the interaction of a fluorescent probe (1-anilino-8-naphthalenesulfonic acid ammonium salt (ANS)) with G3-PMAA was examined by means of fluorescence spectroscopy. As a result, ANS was found to bind to the hydrophobic site of G3-PMAA aggregates at lower pH, and to be released into water phase at higher pH.

1. Introduction

Dendrimers are known to be monodisperse, hyperbranched macromolecules that possess a very high concentration of surface functional groups.[1] A variety of dendrimers have been developed by introducing functionalities into these terminal groups and have been characterized in solution.[2–6] For example, dendrimers terminated with a carbomethoxy group[2] an amino acid,[3] a sugar,[4,5] a perfluoroalkyl[6] or alkyl chain,[7] and an oligo(oxyethylene) segment[8] show encapsulation functions towards guest molecules. Another structural feature of dendrimers is the high degree of control over molecular weight and shape. The diameters of the spherical dendrimers range from 3 to 10 nm. Recently, we have proposed an assembly of oligo-peptides on a dendrimer template as a new approach to model protein structure.[9–11] These oligo(L-glutamic acid)–attached dendrimers have been prepared by a poly(amidoamine) PAMAM dendrimer-initiated polymerization method,[12] and have shown interesting properties such as an enhancement in helicity of the peptide segment and specific encapsulation of α-amino acids. As part of our research into water-soluble oligomer-modified dendrimers, oligo(methacrylic acid)(PMAA) was employed as the oligomer segment in the present study.

PMAA is known to undergo a conformational transition from compact coil to random coil and simultaneously shows a drastic change in hydrophobicity of the segment by varying the surrounding pH.[13] Therefore, if such a PMAA segment can be introduced to a dendrimer surface, the interaction among the resultant dendrimer molecules must be enhanced in aqueous solutions due to hydrophobic interaction. As a result, such a variation in conformation and hydrophobicity of PMAA-attached dendrimer would be expected to lead to be controllable formation of higher-ordered aggregates in aqueous solutions. For this purpose, a novel PMAA-shelled dendrimer (G3-PMAA) has been prepared, which contains the PMAA segment grafted onto the periphery of the third generation PAMAM dendrimer (G3-NH^2) with an ethylenediamine core. The aggregation properties of this dendrimer were examined at different pH values by means of dynamic light scattering. The dendrimer was found to form an aggregate spontaneously in acidic solutions, and its micro-environment was revealed using a fluorescent probe.

2. Results and discussion

2.1. Synthesis and ionization behavior of G3-PMAA

Scheme 1 outlines the pathway for the preparation of G3-PMAA. We have previously reported that poly(methacrylic acid) 'brushes' are successfully grafted onto a two-dimensionally organized monolayer surface by

Keywords: 3rd-generation PAMAM dendrimer; poly(methacrylic acid); living radical polymerization; aggregation; conformational change; encapsulation.

* Corresponding authors. Tel.: +81-774-65-6622; fax: +81-774-65-6844; e-mail: nhigashi@mail.doshisha.ac.jp; mniwa@mail.doshisha.ac.jp.

0040–4020/03/$ - see front matter
doi:10.1016/S0040-4020(03)00469-1

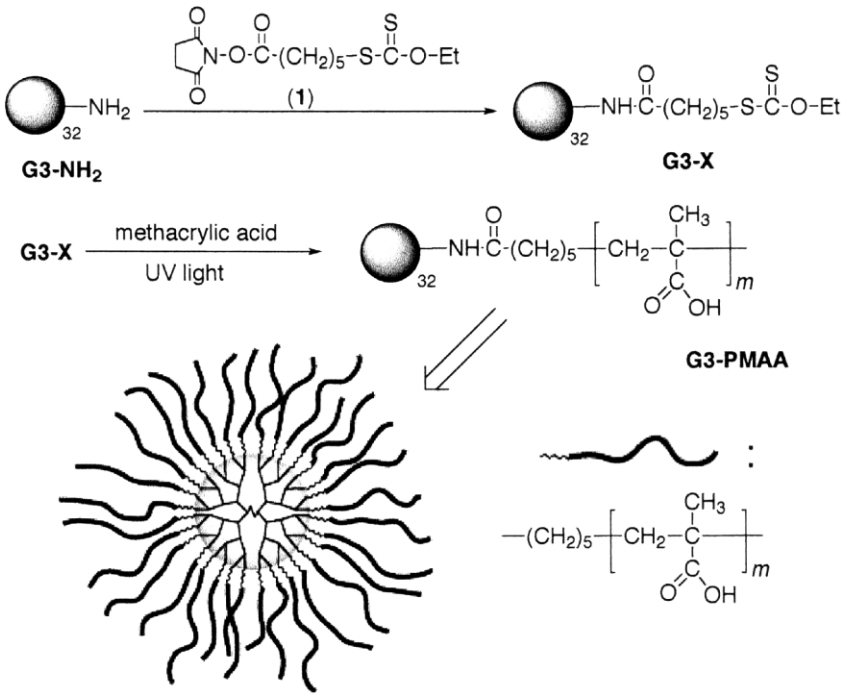

Scheme 1.

photopolymerization.[14] For that purpose, the monolayer surface was modified with a photoactive xanthate group. Xanthate derivatives have been shown to serve as a living radical initiator in the photopolymerization of vinyl monomers.[15] Basically the same procedure was applied to the synthesis of G3-PMAA. The third-generation, amine-terminated PAMAM dendrimer (G3-NH_2) was first allowed to react with 6-*O*-ethyldithio-carbonyl hexanoic acid succinimide with an activated ester moiety. In the presence of this xanthate-modified dendrimer (G3-X), photopolymerization of methacrylic acid was then carried out under UV-irradiation. The polymerized product was characterized by ^{13}C NMR spectroscopies, conductometric titration and size exclusion chromatography. As a result, the graft polymerization was found to proceed from all of the terminal xanthate groups, and the average-degree of polymerization (m) was 10, beyond which the graft segment did not grow, probably because crowded growing radicals would suppress further propagation. For comparison, linear PMAA (L-PMAA) was also prepared using bisisopropyl-xanthogen disulfide, which has played a similar role to the ethylxanthate group,[15] instead of G3-X.

To elucidate the ionization properties of the grafted PMAA segment on the dendrimer, the apparent pK_a value was first of all measured by means of both conductometric and pH titrations. The pK_a value of G3-PMAA (7.3) was found to be somewhat larger than that of L-PMAA (6.8), which is indicative of an interaction among PMAA segments due to grafting onto the dendrimer surface. We have previously reported that the pK_a value of the PMAA segment is considerably enhanced to be 8.5 when it is forced to be aligned two-dimensionally at the air–water interface.[16]

The observed increment in pK_a value for G3-PMAA is not so marked, compared with that for such a two-dimensional monolayer, probably because of the characteristic molecular shape of G3-PMAA, in which the PMAA segments are radially aligned on the three-dimensional core; i.e. there must be a serious difference in the extent of the segment interaction between outer and inner parts in the PMAA shell of the dendrimer.

2.2. Molecular size of G3-PMAA in aqueous solution

PMAA shows a conformational transition from compact coil to expanded structure on elevation of the surrounding pH, reflecting the ionization state of the PMAA segment. It is therefore expected that the particle size of G3-PMAA will

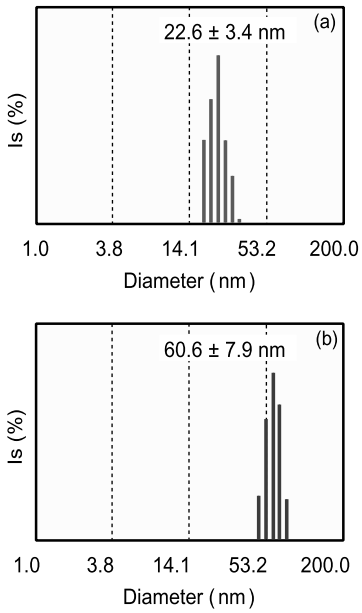

Figure 1. Size distributions of G3-PMMA in aqueous solutions of (a) pH 10.5 and (b) pH 5.8 measured by means of a dynamic light scattering at 20°C. [G3-PMAA]=1.0 mg mL^{-1}.

also be varied due to conformational change of the PMAA segment. Figure 1 shows histograms of size distributions estimated for G3-PMAA at pHs 5.8 and 10.5, at which the PMAA segments have compact coil and expanded conformations, respectively. G3-PMAA reveals unimodal and relatively narrow distributions at both pHs, but its particle diameter is found to vary drastically with pH. Figure 2 displays the pH dependence of the G3-PMAA particle size on the basis of DLS measurements, and in this figure the DLS data obtained at other pHs are also included. The observed diameter in the higher pH region, above pH 10, is about 22 nm. This value is close to the theoretical value (ca. 16 nm) that was calculated by using the diameter of the G3-NH_2 core (3 nm)[11] and the segment length of PMAA taking a completely expanded conformation. Therefore, the G3-PMAA molecules should be in a monomeric state at this pH due to electrostatic repulsive interactions between the deprotonated, anionic PMAA segments. At lower pH, below pH 7, the G3-PMAA diameter had been predicted to be reduced due to contraction of the PMAA chain. Interestingly, the diameter shows a reverse tendency to enlarge with lowering pH. In particular, a steep increase in the diameter is observed at pH 7–8 where the PMAA segment of G3-PMAA has a conformational transition from ionized, expanded coil to compact coil, followed by the change in hydrophobicity of the segment. Below pH 7, the diameter reaches about 60 nm, suggesting formation of an aggregate, composed of several G3-PMAA molecules. When the pH was elevated, the value of diameter returned reversibly to its original one. The same DLS experiments were performed for L-PMAA, and no aggregation was then found to occur over the wide pH range. From these results, it can be concluded that in acidic solution the hydrophobic interaction among compactly coiled-G3-PMAAs is more effectively for self-assembling than that among L-PMAAs probably due to the difference in molecular shape between spherical G3-PMAA and linear L-PMAA.

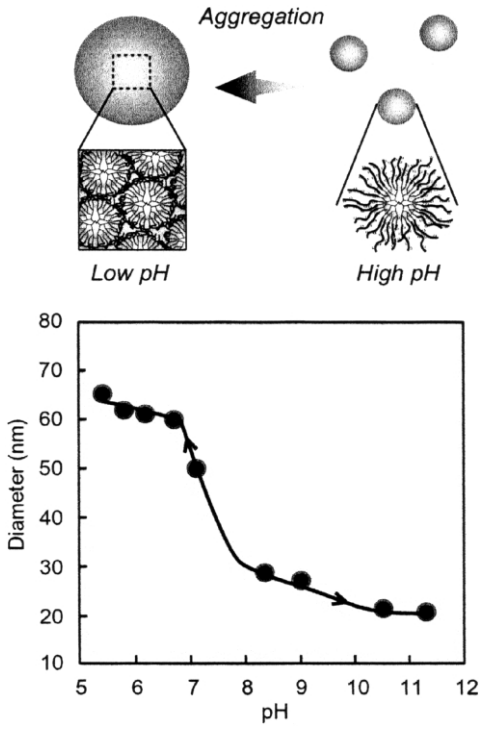

Figure 2. pH Dependence of the diameter for G3-PMAA in aqueous solutions at 20°C. [G3-PMAA]=1.0 mg mL^{-1}.

2.3. Microenvironment and encapsulation function of G3-PMAA

To reveal the microenvironment of these G3-PMAA assemblies and their function as encapsulating agents, 1-anilino-8-naphthalene sulfonic acid ammonium salt (ANS) has been employed in this study, which is a popular anionic, fluorescent molecule to probe the environmental polarity and micro-viscosity. The emission maximum and quantum yield of ANS are known to be very sensitive to the solvent polarity and micro-viscosity.[17] Figure 3 shows fluorescence spectra of ANS in the presence of G3-PMAA, measured at various pHs. It can be seen that the fluorescence intensity increases and the emission maximum (λ_{em}) exhibits a marked blue-shift with decreasing pH. On the basis of these spectral data, λ_{em} and fluorescence intensity are plotted against pH in Figure 4, in which the fluorescence data of ANS in pure water, in aqueous G3-NH_2 and in aqueous L-PMAA solutions are also included. In pure water and in aqueous G3-NH_2 solution, no pH dependence of both λ_{em} and fluorescence intensity is observed, and the values of λ_{em} are in the range of 510–520 nm. The pH dependence of λ_{em} for L-PMAA is somewhat different from those for G3-NH_2 and in pure water; a slight blue-shift of λ_{em} is clearly observed below pH 6, suggesting binding of ANS to the globular-coiled L-PMAA. Further marked pH dependencies of λ_{em} and fluorescence intensity appear in the presence of G3-PMAA. A drastic blue shift of λ_{em} and an increment in fluorescence intensity are observed at lower pH; in particular, below pH 5, such a blue shift of λ_{em} reaches 60 nm, compared to the λ_{em} in pure water.

It has been well-established that a blue shift of λ_{em} and an increment in quantum yield for ANS are induced for decreasing solvent polarity (increasing hydrophobicity) and with increasing micro-viscosity, respectively. The observed spectral changes with pH, therefore, suggest that ANS binds to a more hydrophobic site of G3-PMAA in the lower pH region, where G3-PMAA is aggregated.

In the higher pH region, above pH 7, λ_{em} becomes close to that in pure water although a slight blue shift (about 20 nm) cannot be excluded. This suggests that the bound-ANS

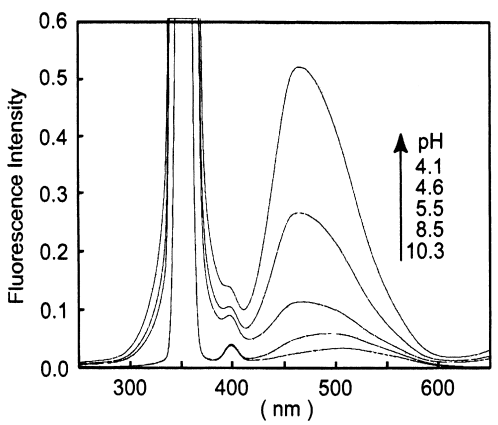

Figure 3. Fluorescence spectra of ANS, excited at 350 nm, in aqueous G3-PMAA at various pHs. [ANS]=4.4×10^{-6} M; [G3-PMAA]=2.2×10^{-6} M.

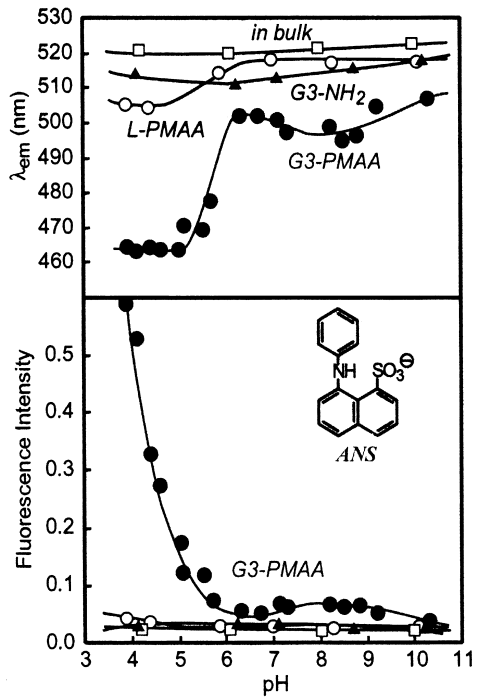

Figure 4. pH Dependence of emission maximum (λ_{em}) and fluorescence intensity of ANS in bulk, aqueous G3-PMAA, aqueous G3-NH_2, aqueous L-PMAA. [ANS]=4.4×10^{-6} M; [G3-PMAA]=[G3-NH^2]=[L-PMAA]=2.2×10^{-6} M.

would be released preferentially into the bulk water phase due to electrostatic interaction between the anionic ANS and deprotonated, anionic PMAA segments. The blue shift, compared to the λ_{em} in pure water, may be assigned to an increase in solution viscosity caused by the addition of G3-PMAA. It should be noted that these spectral changes of ANS in the presence of G3-PMAA were almost completely reversible by varying pH. Fluorescence depolarization (P), which is a useful tool to reveal the surrounding microviscosity of the probe molecule,[11] also supported the above results for pH-dependent ANS-binding properties to G3-PMAA. In the lower pH region (pH 4–6), where PMAA segments take a hydrophobic, compact coil conformation, G3-PMAA spontaneously assembles over each other, and ANS is embedded in the resultant assembly through hydrophobic interaction. When the pH is elevated from pH 6 to pH 11, ANS is released from G3-PMAA to bulk phase due to electrostatic repulsion. This reversible binding and release is controlled at around pH 6. These situations are schematically illustrated in Figure 5.

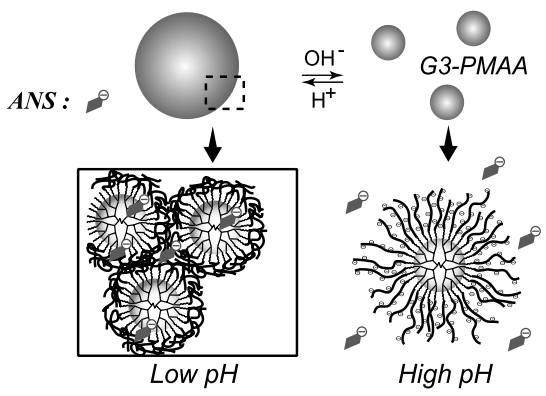

Figure 5. Schematic illustration of microenvironmental change of ANS in G3-PMAA induced with conformational change of the PMAA segment.

3. Conclusions

The present study has described the preparation of a water-soluble PMAA-shelled dendrimer (G3-PMAA) and the relation between ionization and/or conformation of PMAA segments and aggregation properties. The microenvironment of such an aggregate formed in acidic solutions has been revealed using ANS as a fluorescence probe. Consequently, the formation of G3-PMAA aggregates and their binding characteristics with ANS could be controlled by the conformational change of PMAA segments induced with the surrounding pH. We believe that these findings are of importance for a new approach to controlled release systems for small molecules such as pharmaceuticals.

4. Experimental

4.1. General

Methacrylic acid was distilled under a nitrogen atmosphere prior to use, and all other chemicals were reagent grade and used as purchased. Thin-layer chromatography (TLC) was conducted using an Iatroscan TH-10 (Iatron Ltd.) with an FID detector. ^{1}H NMR and ^{13}C NMR spectra were recorded on a JEOL FX400 spectrometer with tetramethysilane (TMS) as an internal standard. The polydispersity (M_w/M_n: M_w, weight-average molecular weight; M_n, number-average molecular weight) of the G3-PMAA was determined by means of size exclusion chromatography (SEC). Size exclusion chromatography was performed in DMSO at 30°C, with a Shimazu Model LC-5A high performance liquid-chromatograph apparatus (column, Shodex KD803 and 804). Conductometric and pH titrations were carried out using a Shimadzu CM-30 and a Hiranuma Comtite-7S, respectively.

4.2. Synthesis of oligo(methacrylic acid)-shelled dendrimer

The oligo(methacrylic acid)-shelled dendrimer (G3-PMAA) was prepared according to Scheme 1.

4.2.1. Synthesis of 6-*O*-ethyldithiocarbonylhexanoic acid succinimide (1). A dichloromethane solution (100 mL) of EDC (1-ethyl-3-(3-dimethylaminopropyl) carbodiimide hydrochloric acid salt)) (4.7 g, 24.3 mmol) was added dropwise to a dichloromethane solution (50 mL) of 6-bromohexanoic acid (3.9 g, 20.0 mmol), *N*-hydroxysuccinimide (2.8 g, 30.0 mmol) and 4-dimethylaminopyridine (0.5 g, 4.0 mmol) in an ice bath, and the mixture was stirred at room temperature. After 14 h, the reaction mixture was washed with water (pH 8) and then dried. After removal of the solvent, 4.4 g (75%) of white powder (6-bromohexanoic acid succinimide) was obtained. R_f (20% MeOH/$CHCl_3$) 0.74; δ_H (400 MHz, C_6D_6): 1.0–1.3 (6H, m, CH_2), 1.7 (4H, b, NCOCH_2), 2.8 (2H, t, BrCH_2), 2.0 (2H, t, CH_2COO).

A mixture of 6-bromohexanoic acid succinimide (4.3 g, 14.8 mmol) thus obtained and sodium *O*-ethyldithiocarbonate

(2.3 g, 16.2 mmol) in acetone (100 mL) was stirred at room temperature for a few minutes in the dark, and then NaBr precipitated was separated. After removal of acetone, the title compound **1** (3.9 g, 80%) as a pale yellow powder was obtained. R_f (20% MeOH/$CHCl_3$) 0.86. The purity was also confirmed by the UV spectrum (λ_{max}=280 nm: $\pi-\pi^*$ transition of SC(=S)O; $\varepsilon_{max}=1.13\times10^4\ M^{-1}\ cm^{-1}$).[15] δ_H (400 MHz, C_6D_6) 1.0–1.3 (6H, m, CH_2), 1.7 (4H, b, NCOCH_2), 2.8 (2H, t, SCH_2), 2.1 (2H, t, CH_2COO), 0.9 (3H, t, *Me*), 4.4 (2H, m, MeCH_2).

4.2.2. Synthesis of photo-active xanthate-modified dendrimer (G3-X). A methanol solution (3 mL) of third-generation poly(amidoamine) dendrimer (G3-NH_2) (1.0 g, 0.15 mmol) was added to a $CHCl_3$ solution (20 mL) of **1** (1.7 g, 5.1 mmol) and the mixture was stirred at room temperature for 4 days in the dark. After removal of the solvent, the residue was washed with acetone several times, giving the title compound G3-X (1.8 g, 89%) as a pale yellow powder. δ_C (100.6 MHz, $CDCl_3$) 215.0, 173.4, 69.9, 52.5, 50.5, 39.5, 37.6, 36.3, 35.9, 34.1, 28.5, 27.8, 25.3, 13.9. The proposed structure for G3-X was also confirmed by the UV spectrum (λ_{max}=280 nm: $\pi-\pi^*$ transition of SC(=S)O; $\varepsilon_{max}=1.13\times10^4\ M^{-1}\ cm^{-1}$).

4.2.3. Polymerization of methacrylic acid initiated with G3-X. The polymerization of a methanol solution (7.7 mL) of G3-X (0.2 g, 1.4×10^{-2} mmol) and methacrylic acid (2.0 g, 23 mmol) was carried out upon UV irradiation with a low-pressure mercury lamp at 30°C in a Pyrex tube under a nitrogen atmosphere after degassing. After 14 h-irradiation, the solvent was evaporated and the residue was washed with benzene, giving a white powder (0.56 g, 18%). δ_C (100.6 MHz, DMSO-d_6) 214.4, 178.1–179.7, 171.2–172.2, 69.9, 52.2, 50.5–53.6, 49.5, 38.4, 36.8, 35.2, 34.9, 33.2, 27.7, 24.6, 13.5. The SEC chromatogram for G3-PMAA thus obtained provided a single peak, and the (M_w/M_n value, which denotes the polydispersity of the grafted PMAA chain, was reasonably narrow; M_w/M_n=1.06. The average-degree of polymerization of PMAA segment (*m*) was evaluated by means of ^{13}C NMR spectroscopy and conductometric titration of COOH groups.

4.3. Dynamic light scattering (DLS) measurement

Samples were filtered through Millex-VV filters (with pore sizes of 100 nm, Millipore Ltd) to remove dust particles in solutions prior to the measurements. Dynamic light scattering measurements were performed in water at 20°C on a DLS 7000 spectrometer (Otsuka Electric Ltd, Japan) equipped with a He–Ne laser (632.8 nm). The pH of the sample solution was adjusted with 1 M HCl or 1 M NaOH. Scattered light from the sample was analyzed at an angle of 90° from incident light. The non-negatively constrained least-squares (NNLS) method was used for correlation analysis to obtain diameter probability distribution functions. The correlation analysis affords directly the diffusion coefficients, from which diameters were calculated using the Stokes–Einstein relationship.

4.4. Fluorescence spectroscopy measurement

Fluorescence spectra were measured on an FP-770 fluorescence spectrophotometer (JASCO Ltd, Japan) equipped with polarizers, at an excitation wavelength of 270 nm. Experiments were performed in a quartz cell with 10 mm path length at room temperature. The fluorescence depolarization value (*P*) was calculated from the following equation:

$$P = (I_{vv} - GI_{vh})/(I_{vv} + GI_{vh})$$

where I_{vv} and I_{vh} are the fluorescence intensities for the vertical and horizontal components when excited with vertically polarized light. *G* is a factor for the instrumental correction (i.e. $G = I_{vh}/I_{hh}$).

Acknowledgements

This work was supported in part by the project 'Hybrid Nanostructured Materials and Its Application' of High Technology Center at RCAST of Doshisha University.

References

1. Tomalia, D. A.; Durst, H. D. *Toc. Curr. Chem.* **1993**, *165*, 193–319.
2. Naylor, A. M.; Goddard, W. A., III; Kiefer, G. E.; Tomalia, D. A. *J. Am. Chem. Soc.* **1989**, *111*, 2339–2341.
3. Jansen, J. F. G. A.; de Brabander-van, E. M. M.; Meijer, E. M. *Science* **1994**, *266*, 1226–1229.
4. Aoi, K.; Itoh, K.; Okada, M. *Macromolecules* **1995**, *28*, 5391–5393.
5. Aoi, K.; Tsutsumiuch, K.; Yamamoto, A.; Okada, M. *Tetrahedron* **1997**, *53*, 15415–15427.
6. Cooper, A. I.; Londono, J. D.; Wignall, G.; McClain, J. B.; Samulski, E. T.; Lin, J. S.; Dobrynin, A.; Rubinstein, M.; Burke, A. L. C.; Frechet, J. M.; DeSimone, J. M. *Nature* **1997**, *389*, 368–371.
7. Chechik, V.; Zhao, M.; Crooks, R. M. *J. Am. Chem. Soc.* **1999**, *121*, 4910–4911.
8. Baars, M. W. P. L.; Kleppinger, R.; Koch, M. H. J.; Yeu, S.-L.; Meijer, E. W. *Angew. Chem. Int. Ed.* **2000**, *39*, 1285–1288.
9. Higashi, N.; Koga, T.; Niwa, N.; Niwa, M. *Chem. Commun.* **2000**, 361–362.
10. Higashi, N.; Koga, T.; Niwa, M. *J. Nanosci. Nanotech.* **2001**, *1*, 309–315.
11. Higashi, N.; Koga, T.; Niwa, M. *ChemBioChem* **2002**, *3*, 448–454.
12. Balogh, L.; Jallouli, A.; Dvornic, P.; Kunugi, Y.; Blumstein, A.; Tomalia, D. A. *Macromolecules* **1999**, *32*, 1036–1042.
13. Olea, A. F.; Thomas, J. K. *Macromolecules* **1989**, *22*, 1165–1169.
14. Niwa, M.; Date, M.; Higashi, N. *Macromolecules* **1996**, *29*, 3681–3685.
15. (a) Niwa, M.; Matsumoto, T.; Izumi, H. *J. Macromol. Sci.-Chem.* **1987**, *A24*, 567–585. (b) Niwa, M.; Sako, Y.; Shimizu, M. *J. Macromol. Sci., Chem.* **1987**, *A24*, 1315–1332. (c) Niwa, M.; Higashi, N.; Shimizu, M.; Matsumoto, T. *Makromol. Chem.* **1988**, *189*, 2187–2199.
16. Niwa, M.; Mukai, A.; Higashi, N. *Langmuir* **1990**, *6*, 1432–1434.
17. (a) Turner, D. C.; Brand, L. *Biochemistry* **1968**, *7*, 3381–3390. (b) Seliskar, C. J.; Brand, L. *Science* **1971**, *171*, 799–800.